A Mutation in Glyceraldehyde 3-Phosphate Dehydrogenase Alters Endocytosis in CHO Cells

April R. Robbins,* Rita D. Ward,* and Constance Oliver[‡]

*Laboratory of Biochemistry and Metabolism, National Institute of Diabetes, Digestive and Kidney Diseases; and [‡]Laboratory of Immunology, National Institute of Dental Research, Bethesda, Maryland 20892

Abstract. The CHO cell mutant FD1.3.25 exhibits both increased accumulation and altered distribution of endocytosed fluid phase tracers. Neither the rate of tracer internalization nor the kinetics of recycling from early endosomes was affected, but exocytosis from late endocytic compartments appeared to be decreased in the mutant. Endocytosed tracer moved more rapidly to the cell poles in FD1.3.25 than in wild type cells. An abundant 36-kD polypeptide was found associated with taxol-polymerized microtubules in preparations from wild type and mutant; in the former but not the latter this polypeptide could be dissociated by incubation of the microtubules in ATP or high salt. The 36-kD polypeptide co-electrophoresed in two dimensions with the monomer of the glycolytic enzyme glyceraldehyde 3-phosphate dehydrogenase (GAPDH). Analysis of cDNA clones showed that the mutant is heterozygous for this enzyme, with ~25% of the GAPDH RNA containing a single nucleotide change resulting in substitution of Ser for Pro_{234}, a residue that is conserved throughout evolution. Stable transfectants of wild type cells expressing the mutant monomer at ~15% of the total enzyme exhibited the various changes in endocytosis observed in FD1.3.25.

THERE are numerous examples in the literature of the presence of the glycolytic enzyme glyceraldehyde 3-phosphate dehydrogenase (GAPDH)[1] in unlikely contexts. Whereas phosphorylation of glyceraldehyde 3-phosphate requires the tetrameric form of the enzyme, the 37-kD monomer functions as a uracil DNA glycosylase (Siegler et al., 1991). Consistent with a role in DNA repair, GAPDH is found not only in the cytosol, where it is an abundant protein, but also in the nucleus (Cool and Sirover, 1989; Morgenegg et al., 1986). A second possible role of nuclear GAPDH is in the export of tRNAs—binding of various tRNAs by the enzyme was shown to correlate with their competence for nuclear export (Singh and Green, 1993).

GAPDH has also been observed to associate with the plasma membrane. In erythrocytes this reflects binding of the enzyme to the cytoplasmic segments of two transmembrane proteins, glucose transporter 1 (Lachaal et al., 1990) and anion exchange protein 1, band 3, (Kliman and Steck, 1980). The latter complexes could be demonstrated in situ in erythrocytes and type A intercalated cells by immunocolocalization performed with sections of kidney medulla

(Ercolani et al., 1992). In studies of skeletal muscle, GAPDH was shown to promote formation of triad junctions from isolated transverse tubules and terminal cisternae of the sarcoplasmic reticulum (Caswell and Corbett, 1985). This activity has been ascribed to the binding of GAPDH to both the dihydropyridine receptor of the transverse tubules and to the junctional foot protein of the terminal cisternae (Brandt et al., 1990). Recent demonstration of binding of two low molecular weight GTP binding proteins to GAPDH associated with the transverse tubules has led to the suggestion of a possible regulatory role of the enzyme in the triad junction (Doucet and Tuana, 1991).

In vitro binding studies have shown that GAPDH associates with filamentous actin (Arnold and Pette, 1970; Méjean et al., 1989), tubulin and microtubules (Kumagai and Sakai, 1983; Durrieu et al., 1987; Walsh et al., 1989; Launay et al., 1989; Somers et al., 1990). Immunostaining of cells permeabilized prior to fixation revealed GAPDH staining consistent with association of the enzyme with stress fibers (Minaschek et al., 1992).

Given the abundance of GAPDH in the cytosol and the dissociation constants measured for the interactions described above, existence of each of these complexes within the cell is plausible, leading one to wonder what the consequences for the cell might be if any of these interactions were altered. In this paper we describe a CHO cell mutant, isolated on the basis of its increased accumulation of a fluid phase endocytic tracer. This mutant exhibits altered distribution of endocytosed tracer and unusual tubulo-

---

Address all correspondence to A. R. Robbins, NIDDK/LBM, 10-9B08, 10 Center Dr. MSC1800, Bethesda, MD 20892-1800. Tel.: (301) 496-2907. Fax: (301) 496-0839. E-mail: cwharr@helix.nih.gov.

1. *Abbreviations used in this paper:* GAPDH, glyceraldehyde 3-phosphate dehydrogenase; LY, Lucifer yellow; SSCP, single-strand conformational polymorphisms; 2-D, two dimensional.

vesicular endocytic compartments. We show that these phenotypic changes result from a single amino acid substitution in a minor fraction of the GAPDH polypeptides, which alters the binding of that enzyme to taxol-polymerized microtubules.

Materials and Methods

Cells and Cell Culture

Cells were routinely grown at 34°C under 5% CO_2 in DME (Biofluids, Inc., Rockville, MD) supplemented with glutamine, non-essential amino acids, penicillin, and streptomycin (all from Biofluids, Inc.) and 5% ultracentrifuged fetal bovine serum (Inovar Laboratories, Inc., Gaithersburg, MD). The isolation of WTB, the parent cells (Thompson and Baker, 1973) and of the ouabain-resistant, thioguanine-resistant derivative of WTB used for hybridization have been previously described (Robbins et al., 1984).

The mutant FD1.3.25 was isolated as follows: WTB was mutagenized with 200 μg/ml ethyl methanesulfonate (Aldrich Chemical Company, Inc., Milwaukee, WI), subcultured for 3 d, and then plated on 10 35 mm dishes (80,000 cells/dish) containing a heat absorbent film lining (Meridian Instruments, Okemos, MI). 3 d later cells were incubated overnight with growth medium containing 2 mg/ml dialyzed FITC-dextran, 40,000 mol wt (Sigma Chemical Co., St. Louis, MO); to chase the label, medium was removed, cells were washed three times and incubated for 2 h in medium without tracer. Cells were then washed with MOPS-FBS buffer (30 mM MOPS, 115 mM NaCl, 5 mM KCl, 1.2 mM $MgCl_2$, pH 7.4, containing 0.1% glucose and 5% FBS). A 2 cm^2 area of each dish was scanned (excitation 488 nm, dichroic 510 nm) using the "Quiklook" option on the ACAS 470 laser cytometer (Meridian Instruments); pixel maps were rescaled based on the fluorescence measured in parallel dishes of WTB cells labeled and chased as above, and then scanned in the absence or presence of 15 mM NH_4Cl; the threshold was set to the former, the high end of the color scale to the latter. Fluorescent "patches" so identified were examined by phase contrast to eliminate those containing rounded, multi-nucleate or out-of-focus cells, all of which apppear fluorescent. Six microcolonies appeared promising and the laser was used in the cookie cutter mode to fuse to the dish an octagon (750-μm diam) of the film liner centered on the microcolony of interest: without disturbing the dish on the microscope stage, buffer was replaced with MOPS containing 25 mM cysteamine; each octagon was cut twice with outer strength, 50%; inner strength, 25%; 1 inner killing ring of radius 250 μm, laser power, 200 mW; stage speed, 0.25 mm/s. Dishes were rinsed several times with growth medium, their perimeters swabbed to remove cells not on the film liner, they were rinsed several times more, then the film liners were removed, dishes were rinsed again, swabbed again, rinsed again and returned to 34°C; all of the above were performed under sterile conditions.

Three days later cells remaining on the dishes were again incubated overnight with FITC-dextran, the label was chased for 2 h, and then the cells on or in the immediate vicinity of each octagon were analyzed for cell-associated fluorescence, with the area covered by a single scan just exceeding that of the octagon. Two of the six original octagons contained about 50 cells with cell-associated fluorescence greater than that measured in parallel scans of WTB cells. Cells on these octagons were picked from the master dishes, amplified and cloned by limiting dilution.

Clonal populations were tested after overnight incubation with FITC-dextran followed by a 2-h chase: each 35 mm dish was examined under low levels of visible light and 25–30 cells in the same focal plane in non-overlapping fields were chosen based on representative morphology and separation of ≥3 μm from neighboring cells. Positions of these cells were listed. Fluorescence of the selected fields was scanned automatically in 0.5-μm steps; each scan required ∼1 min. The scan strength employed resulted in no detectable photobleaching after 10 repeated scans. To analyze the results, the false color images of labeled cells were rescaled such that each cell could be seen in its entirety on the basis of its intrinsic fluorescence; any cell or portion thereof other than the cell of interest was excised from the image. The total fluorescence of the remaining image was determined by summing the pixel values after correcting each pixel by subtraction of a background value based on the maximum value of an individual pixel obtained on parallel scans of unlabeled cells. Cells from 7 of the 29 clones obtained from one of the octagons (FD1.3), exhibited cell-associated fluorescence uniformly higher than that measured with WTB;

they also exhibited similar morphological alterations (see Fig. 1). One of these clones is FD1.3.25.

Assays of Endocytic Activity

For measurements of accumulation of FITC-dextran in individual cells, cells were plated on 35 mm dishes 3 d prior to testing. Cells were incubated with dialyzed FITC-dextran, 2 mg/ml in growth medium, for 1 h, washed three times and incubated for 2 h in tracer-free medium. Cells were rinsed with 2 ml MOPS-FBS, and then analyzed in 1 ml of this buffer. Fluorescence of 25–30 individual cells was assayed as described above. When all of the selected fields had been scanned, to assess cell-associated fluorescence after alleviation of quenching that occurs at acidic pH, 1 ml of MOPS-FBS containing 50 μM monensin (Calbiochem-Behring Corp., La Jolla, CA) was added without disturbing the dish on the microscope stage. After 5 min the selected fields were again scanned automatically. Images of each cell both before and after monensin were analyzed as described above. The level of accumulation of FITC-dextran in a cell was the value obtained in the presence of monensin.

Assays of accumulation in individual cells of Lucifer yellow (LY), obtained from Molecular Probes (Eugene, OR), were similar to those described above, except that cells were incubated in the tracer in serum-free medium containing 0.1% BSA and that cells were fixed prior to analysis by rinsing twice quickly in PBS (37°C), and then incubated in 2% formaldehyde in PBS (37°C) for 30 min at room temperature. Cells were rinsed with PBS following fixation, and then analyzed in PBS.

For assays of accumulation of FITC-dextran in populations, cells in 6-well trays were pulsed and chased with FITC-dextran as above, and then rinsed with DPBS, removed from the wells with 0.5 ml of 0.1% trypsin in DPBS, then mixed with 0.5 ml of MOPS-(20%) FBS. Fluorescence was measured in a Farrand Ratio-2 Fluorometer (Optical Technology Devices, Inc., Elmsford, NY) using 490- and 525-nm narrow band path interference filters for excitation and emission, respectively. Monensin was then added to 25 μM and fluorescence remeasured. Cell number was determined for each sample; fluorescence values were corrected by subtraction of background measured with unlabeled cells and data was normalized to cell number.

The assay of transferrin recycling was a minor variation of previously described procedures (Klausner et al., 1984; Yamashiro et al., 1984). Cells grown for 3–4 d in six-well trays, 35-mm wells, were rinsed three times in serum-free growth medium containing 0.1% BSA, and then incubated with ^{125}I-Tf 10 μg/ml, for 60 min at 34°C. Cells were rapidly washed three times in tracer-free medium, then medium containing 1 mg/ml transferrin and 100 μM desferrioxamine (Ciba-Geigy Corp., Greensboro, NC) was added to initiate the assay. At intervals cells were rinsed three times quickly with cold PBS, then solubilized in 0.1 M NaOH and counted in a Beckman 9000 gamma counter. Values were corrected for non-specific binding and uptake, determined by incubation in the presence of 1 mg/ml transferrin, then normalized for cell protein, determined using the BCA™ protein assay reagents (Pierce, Rockford, IL).

Internalization was measured using HRP type VI (Sigma Chemical Co.). Cells in six-well trays (35-mm wells) were equilibrated in three changes of Hepes-buffered Ringer's solution, pH 7.2, containing glucose and BSA (formulated as described in Heuser, 1989) for 15 min in a CO_2-free incubator (37°C). Pre-warmed solutions of HRP, 2 mg/ml in Ringer's, were added to the cells to initiate the assay. At various time points cells were washed, lysed and assayed following the procedures of West et al. (1989). Enzyme activity was linear over the range of 0.25–10 ng/ml in the final assay mixture. Internalized tracer was normalized to cell protein. Background activity (HRP bound to the cell surface or the dish) was measured both by incubation of cells with the tracer at 0°C and by adding and immediately removing HRP at 37°C; the two procedures gave virtually identical results, 0.84 ± 0.05 ng/100 μg cell protein, with the various cell types assayed.

Fluorescence Microscopy

Cells were plated on Permanox® two chamber slides 3–4 d prior to experiments. Prior to incubation with tracer, cells were equilibrated in an incubator without CO_2 by washing three times over 15 min in Hepes-buffered Ringer's solution, pH 7.2, containing BSA and glucose (formulated as described in Heuser, 1989). Incubation with endocytic tracers and chase of the label was also performed in this solution. To remove extracellular tracer following the pulse, cells were rapidly rinsed three times. For fixation cells were quickly rinsed two times in PBS, 37°C, and then 2% formaldehyde in PBS, 37°C, was added for 30 min at room temperature. Follow-

ing fixation cells were rinsed four times in PBS. Coverslips were mounted in Fluormount-G (Southern Biotechnology Associates, Inc., Birmingham, AL) that had been diluted in PBS. Cells were viewed with a Nikon Microphot-FX fluorescence microscope.

Electron Microscopy

Cells were plated in six-well trays 3 d prior to the experiments. Cells were rinsed three times in serum-free growth medium supplemented with 0.2% BSA then incubated for 30 min in 2 mg/ml HRP (type VI) at 34°C. Following three quick rinses in serum-free medium and two in PBS cells were fixed in 1% glutaraldehyde -1% formaldehyde for 60 min at room temperature. The samples were rapidly rinsed five times in PBS, once in 0.1 M glycine, pH 7, and then incubated for 45 min in a 0.019% hydrogen peroxide-DAB (0.94 mg/ml) solution prepared in 0.1 M cacodylate buffer, pH 7.4. Following a wash with cacodylate buffer, cells were postfixed in 2% potassium ferrocyanide-reduced osmium tetroxide (Karnovsky, M. J. 1971. *J. Cell Biol.* 51:146a) for 1 h, and then washed extensively in cacodylate buffer. Samples were dehydrated through a graded series of ethanols, then cells were removed from the plate with propylene oxide. After three or four quick washes in acetone the samples were embedded in Spurr's embedding media (Spurr, 1969). Thin sections were cut with a diamond knife, collected onto copper grids, and examined in a JEOL 100C electron microscope. Photomontages were prepared to illustrate the entire cell and provide spatial information on distribution of labeled vesicles. This procedure was chosen because the 5,000× magnification negatives used to create the photomontages provide higher resolution upon enlargement than those of lower magnification in which the entire cell is recorded on a single negative.

Preparation and Analysis of CHO Cell Microtubule Proteins

The method used is derived from that described by Vallee, 1982. Cells were grown for 3 d on 150 mm dishes plated at 2×10^6 cells/dish. For radiolabeled material cells on one dish (out of four to eight) were incubated 12–16 h with [^{35}S]methionine at 50 μCi/ml in medium containing reduced (1.2 μg/ml) methionine. Label was chased for 30 min prior to harvest. Dishes were placed on ice, cells were rinsed three times, and scraped in cold PBS, washed three times by centrifugation at 1,000 g, 4°C, and then resuspended at 1.5 times packed cell volume in microtubule buffer: 100 mM Pipes, pH 6.9 containing 1 mM MgCl$_2$, 1 mM EGTA, 1 mM DTT, aprotonin (0.1 TIU/ml), leupeptin (1 μg/ml), and pepstatin (1 μg/ml). Cells were lysed by sonication on ice, lysates were centrifuged for 20 min at 38,000 g, 4°C, and then the supernates were centrifuged for 90 min at 100,000 g, 2°C. Aliquots were taken from the final supernate for measurement of A$_{280}$ and radioactivity, then taxol (20 μM) and GTP (1 mM) were added. (Henceforth in the procedure all buffers contain taxol and GTP; taxol was provided by the Drug Synthesis and Chemistry Branch, Developmental Therapeutics Program, Division of Cancer Treatment, NCI). The solution was distributed into 1.5 ml microfuge tubes (material from approximately two dishes per tube), and incubated for 25 min at 37°C, the contents of each tube was then layered onto 5% sucrose in 0.3 ml microtubule buffer and centrifuged at 38,000 g for 20 min at 30°C. The pellets obtained were either solubilized for examination of initial microtubule pellets, or washed by centrifugation, first in microtubule buffer, then in microtubule buffer containing 0.4 M NaCl or 1–2 mM ATP; in the latter case buffer was supplemented with compensatory MgCl$_2$.

Pellets were solubilized by addition of 0.1 ml SDS solubilizer (62.5 mM Tris, pH 6.8, 10% glycerol, 2.5% SDS, 5% mercaptoethanol) that had been heated to 95°C, and stored at -80°C. For analysis by SDS-PAGE 5–10 μl were electrophoresed on pre-cast 4–12 or 8–16% Tris-glycine gels (NOVEX, San Diego, CA). For two-dimensional (2-D) gel electrophoresis 20 μl of the sample was precipitated by addition of 10 vol of ice-cold acetone containing NH$_4$OH, 5.3:0.3 (Cabral and Gottesman, 1978). After the pellet had dried it was dissolved in 50 μl of freshly prepared 2-D dissociation buffer (1.08 g urea added to 0.96 ml of 5 mM Tris, pH 7.0, 0.5 mM EDTA, 0.5 mM EGTA, 0.05% NP-40, plus 0.1 ml mercaptoethanol). To each sample was added an equal volume of lysis buffer (O'Farrell, 1975) then samples were loaded on NEPHGE tube gels prepared with pH 3.5–10 Ampholines (Pharmacia LKB Biotechnology, Inc., Piscataway, NJ) and electrophoresed from anode to cathode for 4 h at 400 V at 20°C, all as described (O'Farrell et al., 1977). Gels were extruded into SDS solubilizer, incubated with rocking for 2 h at 25°C, and then frozen quickly in ethanol-dry ice and stored at -80°C. Electrophoresis in the second dimension was on a Tris-Glycine polyacrylamide 8–12% exponential gradient

gel (O'Farrell, 1975), with a 4% stacking gel, both containing 0.1% SDS. Gels were fixed in 15% trichloroacetic acid, and then subjected to fluorography (Bonner and Laskey, 1974).

Molecular Genetics

All oligonucleotides were from Midland Certified Reagent Co. (Midland, TX); all restriction enzymes from New England Biolabs (Beverly, MA). To generate GAPDH cDNA, mRNA was isolated from WTB and FD1.3.25 using a Fast Track™ mRNA Isolation Kit (Invitrogen Corp., San Diego, CA). Reverse transcription of the mRNA was primed with random hexamers and was carried out using the Gene Amp™ RNA PCR kit (Perkin Elmer Cetus, Norwalk, CT). PCR (Mullis and Faloona, 1987) was primed with 24-mer oligonucleotides corresponding to the 5' and complementary to the 3' ends of the coding sequence (nucleotides 74–97 and 1049–1072, respectively) published for hamster GAPDH cDNA (Vincent and Fort, 1990) and was carried out for 30 cycles of 95°C, 2 min; 60°C, 1.5 min; 72°C, 2 min. The cDNAs obtained from parent and mutant coelectrophoresed at 1 kb. These PCR products were cloned directly into Bluescript KS (Stratagene, La Jolla, CA) that had been modified to a T vector following the procedure of Marchuk et al. (1991).

Analysis of cDNA. Orientation of inserts in the vector was determined by digestion with HindIII. cDNAs were then compared for single-strand conformational polymorphisms (SSCP), using the published procedure (Orita et al., 1989) with the minor modifications noted below. cDNAs were amplified as segments of 300–400 bp using as primers 20-mer oligonucleotides, end-labeled with [γ-^{32}P]ATP (~6,000 Ci/mmol) and T4 polynucleotide kinase. 100 ng of plasmid, 100 pmole of each primer (diluted with cold primer to 1×10^6 cpm/100 pmole), 2.6 mM MgCl$_2$, 2.5 U of Taq polymerase, and 0.2 mM of each deoxynucleotide were used in the amplification, run for 12 cycles of 95°C, 2 min; 50°C, 1.5 min; 72°C, 2 min. Samples were prepared and electrophoresed on 6% polyacrylamide gels containing 10% glycerol as described in Orita et al. (1989), except that electrophoresis was for 10–12 h at 30 W. Sequencing of the plasmid inserts was by the dideoxy chain termination method (Sanger et al., 1977) using Sequenase Version 2.0 (United States Biochemical, Cleveland, OH) and the primers employed above for PCR-SSCP.

Cloning of GAPDH cDNA$_{FD}$ into the mammalian expression vector pcDL-SRα296 (Takebe et al., 1988), modified by inclusion of a polylinker, is summarized as follows: First, a 5' fragment of the cDNA containing a NotI restriction site and a Kozak translation initiation site (Kozak, 1987) was generated by PCR using as sense primer 5' TTT AAG TAT GCG GCC GCC ACC ATG GTG AAG GTC GGC GTG AA 3', the last 20 nucleotides of which correspond to the first 20 nucleotides of the coding sequence, and as antisense primer an internal sequence complementary to nucleotides 298–317 of the coding region. Similarly, a 3' fragment containing a termination codon and an XbaI site was generated with a sense primer corresponding to nucleotides 604–623 of the coding sequence and an antisense primer 5' GTA TTT AAG AAT TCT AGA TTA CTC CTT GGA GGC CAT GTA 3' whose last 18 nucleotides complement the final nucleotides of the coding sequence. Each of the resultant amplified segments contained a restriction site present once in hamster GAPDH cDNA (and absent from Bluescript): BstEII at position 45 and SfiI at 985. Each PCR product was cut with the appropriate enzyme, and a sequenced GAPDH$_{FD}$ cDNA clone was cut sequentially with SfiI then BstEII. Following digestion the three fragments (5' 69 bp, middle 940 bp, 3' 34 bp) were ligated (Struhl, 1985), and then cloned into pcDL-SRα296 by sequential digestion of both the ligation product and plasmid with NotI and XbaI. Note that between each of the steps of this procedure, the material was subjected to some form of purification: Magic PCR Clean-Up, Magic DNA Clean-Up (Promega, Madison, WI) or electrophoresis then excision from agarose gels.

Cloned plasmids were tested by double digestions, first with NotI and XbaI, second with SfiI and BstEII. Clones were further checked by sequencing, using for the 5' end an anti-sense primer complementary to nucleotides 81–100 of the coding sequence, and at the 3' end a sense primer corresponding to nucleotides 921–940. This allowed verification of the recombinant cDNA from positions within the 940-bp middle segment of the GAPDH cDNA, through the segments obtained by PCR and on into the vector.

To generate stable transfectants pcDL-SRα296 and pcDL-SRα296-GAPDH$_{FD}$ were linearized with ScaI, and pRc/CMV (Invitrogen Corp.) was linearized with PvuI. Following digestion DNAs were put through Magic DNA Clean-Up. WTB cells (1×10^7/T175 flask) were harvested by trypsinization, washed twice with PBS, and then resuspended in "cytomix" (formulated as described in van den Hoff et al., 1992) to 1.25×10^7
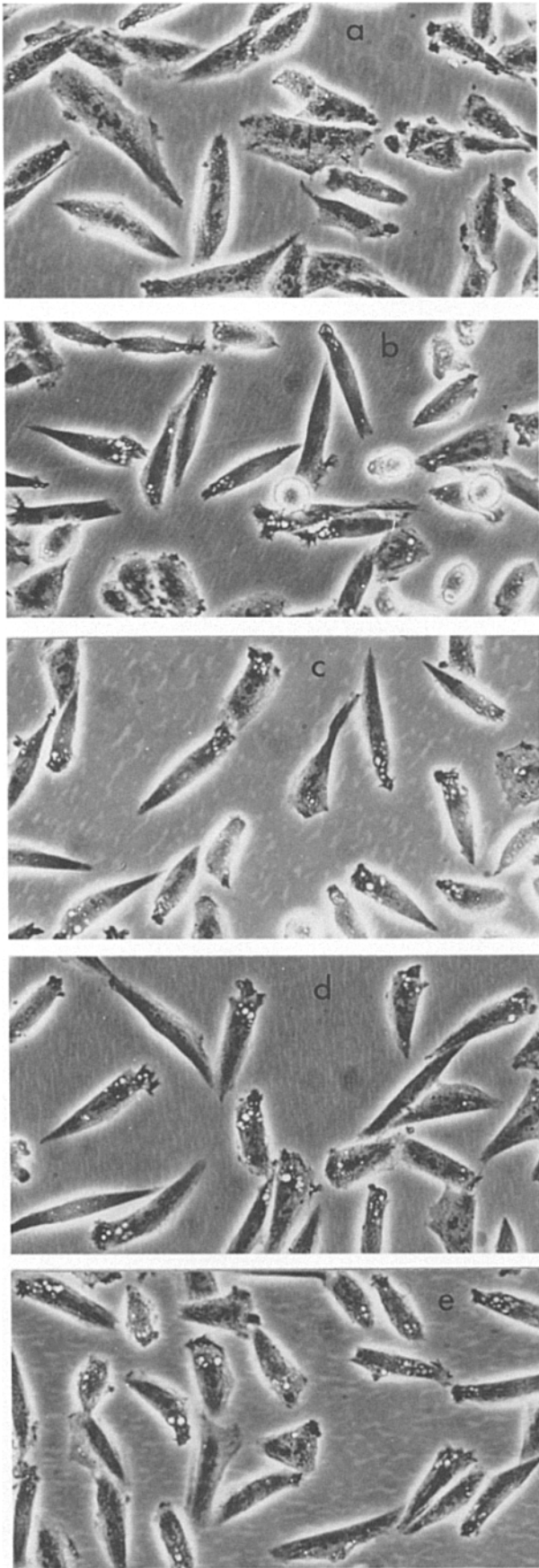
Figure 1. Morphology of WTB, the mutant FD1.3.25, and three independent clones of WTB stably transfected with GAPDH$_{FD}$

cells/ml. Aliquots of 0.35 ml were placed in 4-mm electroporation cuvettes; 12 μg of pcDL-SRα296 or its GAPDH$_{FD}$ derivative and 2.5 μg of pRc/CMV were added to the cuvettes; electroporation was performed at 290 V, 960 μF. Cells were diluted and plated for selection and measurements of viability by colony formation (65–80% untreated controls); after 48 h G418 (GIBCO BRL, Gaithersburg, MD) was added to the growth medium at 800 active μg/ml. After 14 d colonies were picked, amplified, tested as described below, and then cloned by limiting dilution.

To determine the presence of GAPDH RNA containing the mutation, cells were grown in duplicate on 12-well trays, and then RNA was extracted using a Micro-scale Total RNA Separator Kit (Clontech Laboratories, Inc., Palo Alto, CA). Yields ranged from 10–16 μg/well. RNA (1 μg) was reverse transcribed for 1 h, and then a segment of the cDNA was amplified using as sense primer an oligonucleotide corresponding to nucleotides 604–623 of the coding sequence and an anti-sense primer complementary to 979–1002. Amplification was for 30 cycles of 95°C, 2 min; 53°C, 1.5 min; 70°C, 2 min. Samples were tested by allele specific hybridization, following the procedure of Myerowitz (1988), using as probes ^{32}P-labeled 15-base oligonucleotides, CCGTGTTCCTACCCC and CCGTGTTTC-TACCCC, corresponding to nucleotides 693–707 of the wild type and mutant sense strands, respectively. Temperatures used for differential separation were 47° and 45°C for wild type and mutant probes, respectively. Following exposure to film, results were quantitated by cutting the blots (3/4-in squares surrounding the spots) and measuring the Cerenkov radiation; following subtraction of background and correction for any difference in the specific activities of the probes, ratios of GAPDH$_{FD}$/total GAPDH were calculated.

Results

The mutant FD1.3.25 was identified because it exhibited greater cell-associated fluorescence than wild type cells following an overnight incubation with FITC-dextran (see Materials and Methods). As compared to its parent, WTB (Fig. 1 *a*), FD1.3.25 (Fig. 1 *b*) has an unusual appearance, manifesting an active surface ruffle(s), with many clear vacuoles in the cytoplasm behind the ruffled edge. The nature of these vacuoles is unknown; although they are often closely apposed by endocytic compartments, they do not contain endocytosed tracer at any time (10 min to 20 h) following internalization. They are not acidic, based on lack of staining with acridine orange. These vacuoles are less refractile than the occasional lipid droplet observed in both mutant and parent cells, and they fail to stain with either Oil red O or fillipin. Casual observation suggests that the vacuoles move slowly outward to the ruffle, then disappear (data not shown). Cells in Fig. 1 (*c–e*) will be discussed in a later section.

Endocytosis

Various aspects of endocytic activity in WTB and FD1.3.25 are compared in Table I. The increased fluorescence of intracellular FITC-dextran for which the mutant was isolated reflects elevated accumulation of fluid phase tracers: After a 1-h pulse, 2-h chase with FITC-dextran or LY, measurements of individual cells showed ∼2.7 times more intracellular tracer in FD1.3.25 than in parental cells. Measurements of cell populations labeled in identical fashion showed a ∼2.4-fold increase in the mutant.

In the mutant following the 1-h pulse, 2-h chase fluid phase tracer is located in lysosomes. Fractionation of ho-

cDNA. 4 d after plating cells were fixed in 2% formaldehyde-0.5% glutaraldehyde in PBS for 30 min at room temperature and photographed in PBS-0.1% BSA: in contrast to WTB (*a*), FD1.3.25 (*b*) and the transfectants 1B (*c*), 5C (*d*), and 9C (*e*) manifest active surface ruffles and vacuoles behind the ruffled edge.

Table I. Comparison of Endocytic Activities in Parental and Mutant Cells

	WTB	FD1.3.25
Tracer accumulation*		
1-h pulse, 2-h chase		
FITC-dextran	1	2.8 (2.4–3.3)
LY	1	2.7 (1.7–3.7)
HRP internalization[‡]		
3 min	2.8 ± 0.2 ng	2.7 ± 0.2 ng
6 min	7.0 ± 0.5	7.2 ± 0.6
9 min	10.5 ± 1.0	10.3 ± 1.0
30 min	22.1 ± 0.7	29.0 ± 1.6
Tf recycling[§]		
$t_{1/2}$	10.0 ± 1 min	10.0 ± 1 min
LY Recycling[‖]		
30-min pulse	1	1.3 (1.1–1.6)
1-h chase	0.60 (0.52–0.77)	1.2 (0.9–1.5)
2-h chase	0.44 (0.26–0.63)	1.1 (0.9–1.4)

Details of each assay procedure are presented in Materials and Methods.
*25–30 cells in each of 5 (FITC-dextran) or 4 (LY) experiments were selected for analysis by phase contrast microscopy. To minimize day to day variation, the average fluorescence (arbitrary units) was calculated for each cell type in an individual experiment and the mean obtained for the mutant was normalized to that of the parent. The value given is the mean of these normalized means. The values in parentheses represent the range obtained with individual cells—in each experiment wild type and mutant cells were ranked in order of increasing fluorescence, then the value of each mutant cell was normalized to the value of the corresponding wild type cell.
[‡]Results are from three experiments with duplicate samples for each time point, and are corrected for background determined as described in Materials and Methods, and then normalized to 100 µg cell protein.
[§]Results are from three experiments with triplicate samples for each time point. Cells were incubated with ^{125}I-Tf for 60 min prior to initiation of the assays; at this time cell-associated Tf was 5,400 ± 400 and 5,500 ± 300 cpm/100 µg in WTB and FD1.3.25, respectively. Samples were taken every 10 min; exocytosis followed first-order kinetics in both cell types.
[‖]Results presented are from four experiments, with 25–30 cells for each sample in each experiment. Values were calculated as described above, except that means were normalized to the mean obtained for wild type cells pulsed for 30 min. Values in parentheses again represent the range obtained with individual cells, normalized to the value of the corresponding wild type cells in the 30-min sample.

mogenates prepared from WTB and FD1.3.25 on 26% Percoll gradients showed 80–90% of the FITC-dextran in both cell types sedimenting with dense lysosomes. In these lysosomes, levels of four acid hydrolases (α-mannosidase, β-galactosidase, β-glucuronidase, and β-hexosaminidase) were the same in wild type and mutant cells.

Increased accumulation of fluid phase tracer can result from increased uptake, decreased exit (retroendocytosis), or a combination of both. Rates of internalization, measured with HRP, were similar in mutant and parent (Table I), leaving decreased exit of internalized tracer as the remaining possibility. However, measurements of transferrin recycling in parent and mutant gave identical results, indicating that exocytosis from the early portion of the endocytic pathway was unaffected in FD1.3.25. Increased accumulation in the mutant appears to result from decreased exit of fluid phase tracer from compartments beyond the early endosome. As shown in Table I, the levels of intracellular tracer were similar in WTB and FD1.3.25 following a 30-min pulse (1 and 1.3, respectively), but after 1 h of chase the parent had lost ~40% of the tracer and after 2 h, 55%, whereas the mutant retained ≥85% over this time.

Distribution and Morphology of Endocytic Compartments

Although WTB and FD1.3.25 contained similar amounts

of tracer after the 30-min pulse, false color images generated from these samples indicated a different distribution of labeled compartments in the parent and mutant cells. Tracer appeared to be randomly distributed throughout the cytoplasm of the parent, whereas in the mutant labeled vesicles were concentrated at one or both poles of the cell (data not shown). This polar localization reflects vesicle redistribution subsequent to tracer internalization. After a 10-min pulse and 5-min chase of LY, both parent (Fig. 2 a) and mutant (Fig. 2 c) cells showed labeled vesicles scattered throughout the cytoplasm. After a 15-min chase, most of the tracer in FD1.3.25 was clustered at the poles (Fig. 2 d), whereas little change in distribution was observed in WTB (Fig. 2 b). After 30 and 45 min of chase ~50 and 90%, respectively, of WTB cells exhibited some polar clustering of tracer, albeit to a lesser extent than that observed in FD1.3.25 after 15 min. No polar labeling was observed in either cell type when FITC- or Texas red–transferrin was used as the endocytic tracer in either continuous pulses or pulse–chase incubations (data not shown).
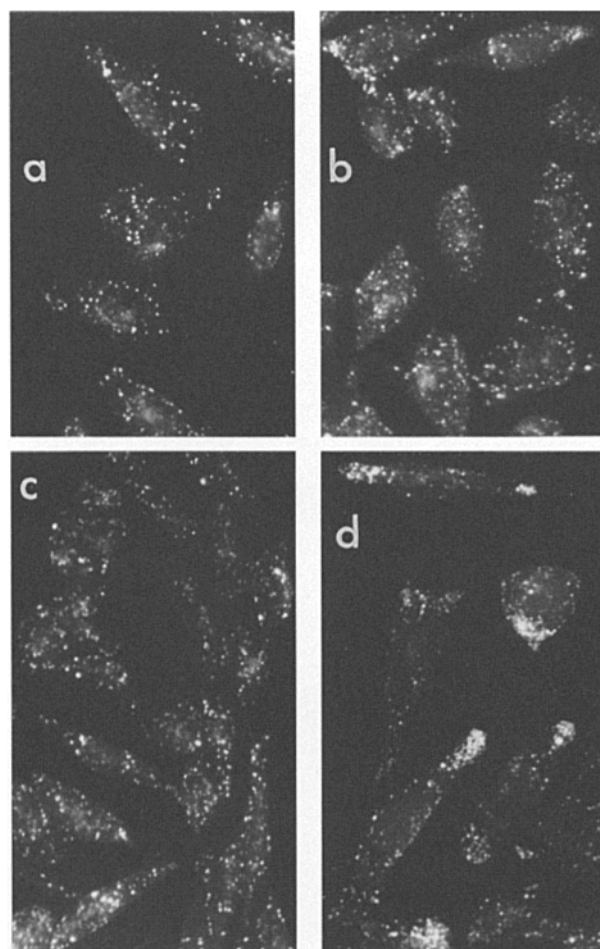

Figure 2. Fluid phase tracer is translocated to the cell poles subsequent to internalization; polar localization requires intact microtubules. After incubation of WTB (a and b) and FD1.3.25 (c and d) with LY for 10 min, tracer was chased for 5 min (a and c), or 15 min (b and d). Following the 5-min chase LY appears randomly distributed in both cell types; after the 15-min chase most of the tracer is clustered at the poles of the mutant, but remains scattered in the parent.
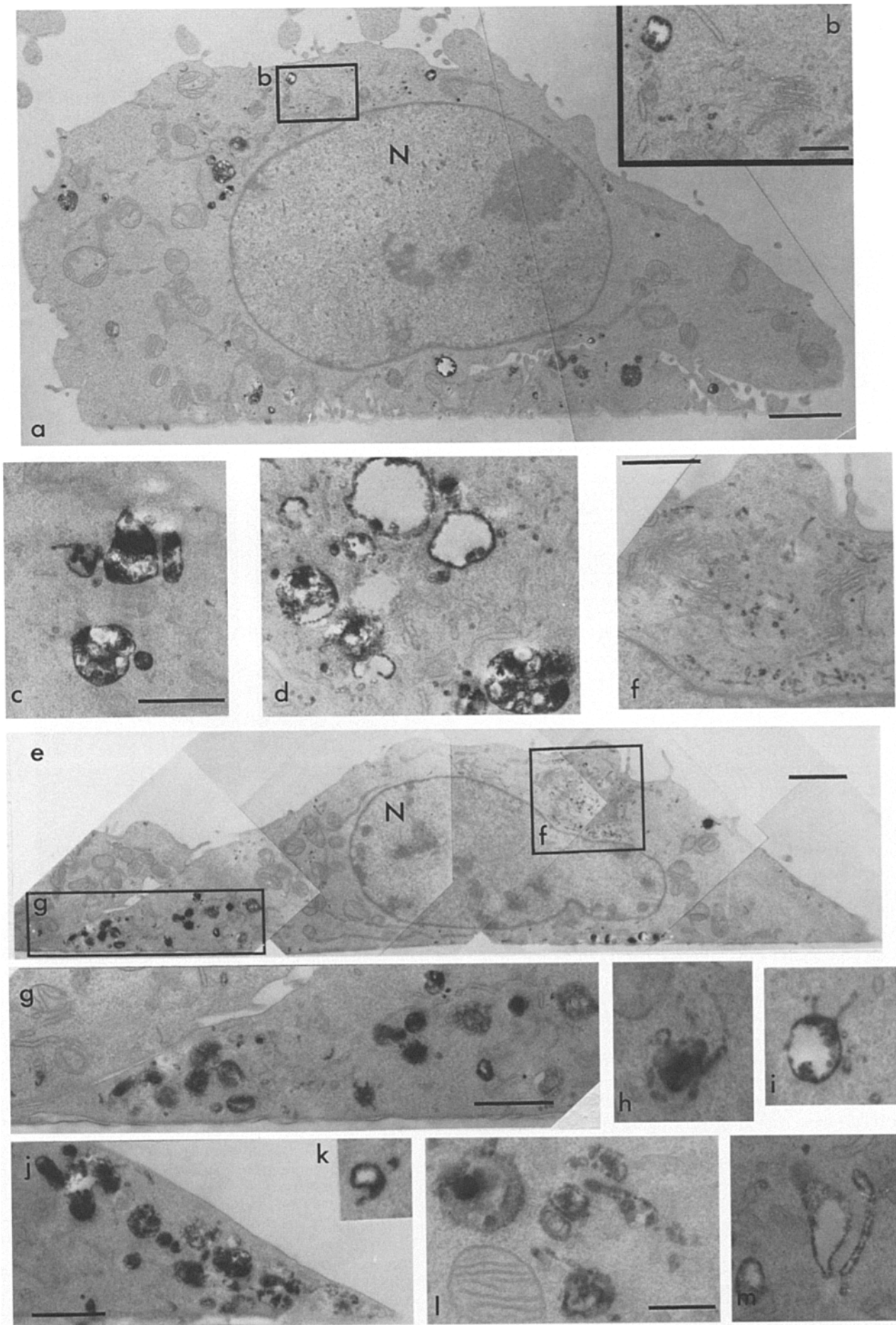
WTB and FD1.3.25 were examined under the electron microscope after a 30-min pulse with HRP (Fig. 3). As was observed by light microscopy, there is a dramatic difference in tracer distribution in parent (Fig. 3 a) versus mutant (Fig. 3 e) cells. A congregation of mainly large (0.8–1.3 μm) endocytic vesicles, including multivesicular bodies, was frequently observed at one end of the mutant cells (Fig. 3, e, g, and j); this distribution was not observed in parental cells. The characteristic vacuoles of FD1.3.25 (Fig. 1 b) do not preserve well under the conditions used for electron microscopy; where found, they are clearly devoid of tracer or any other detectable material (data not shown). Both cell types have small (80–160 nm) labeled vesicles distributed throughout the cytoplasm, with an increased concentration in the vicinity of the Golgi complex (Fig. 3, b and f). Vesicles at the lower end of this size range are sometimes arranged in tandems of up to eight vesicles, resembling tubules. In no case was label observed in the Golgi complex. The morphology of medium-sized (160–800 nm) vesicles also differed in parent and mutant. In the former these round vesicles exhibited a uniform periphery (Fig. 3, c and d), whereas in the latter, vesicles at the higher end of the size range (400–800 nm) often manifested tubular extensions (average length 430 nm), giving them a characteristic comma or swan shape (Fig. 3, h, i, k, l, and m). As shown in Fig. 3 (h and i), these compartments frequently appear to be surrounded by smaller labeled vesicles, which may be additional tubular extensions outside the plane of section. Vesicles of this type were common enough to be found in nearly every section of the mutant cells, whereas examination of as many or more sections of WTB revealed a single example of this structure (Fig. 3 c). In FD1.3.25 following a 10-min pulse HRP also appeared in these odd-shaped vesicles, albeit they were less frequent (data not shown).

In other experiments cells were examined after various times of pulse or pulse–chase with transferrin-HRP (data not shown). In both WTB and FD1.3.25 after a 40-min pulse most of the tracer was found concentrated near the Golgi complex in small vesicles or long tubular compartments similar to those shown in Fig. 3 (b and f). In contrast to HRP, transferrin-HRP was not observed in vesicles with tubular extensions, nor at the cell poles in the mutant. Unlike transferrin, HRP can survive for hours in the late endosomal/lysosomal environment; thus, the absence of transferrin-HRP from these compartments in the mutant seems indicative of lack of movement of transferrin to, rather than degradation of transferrin within those compartments.

Proteins Binding Taxol-polymerized Microtubules

A variety of observations (manuscript in preparation) sug-

gested that microtubule-dependent movement of endocytic vesicles in FD1.3.25 might be altered. Thus, it seemed reasonable to look among microtubule-associated proteins for the affected protein. We compared the proteins present in taxol-polymerized microtubules from parent and mutant. No reproducible difference was observed on examination of initial microtubule pellets by SDS-PAGE, but when these pellets were washed with 0.4 M NaCl or 2 mM ATP, a polypeptide electrophoresing at ∼36 kD was observed in preparations of the mutant but not the parent (Fig. 4). A rather prominent polypeptide of 36 kD was present in the initial microtubule pellets from both cell types; analysis of the various pellets by 2-D gel electrophoresis showed that a 36-kD polypeptide of basic pI is lost from the microtubule pellet of WTB cells after incubation with salt (Fig. 5) or ATP (data not shown) but remains in the pellets from FD1.3.25. Microtubule pellets prepared from stable WTB × FD1.3.25 hybrids contained this same polypeptide after washes with salt or ATP (data not shown), suggesting that altered binding of the protein is dominant. Polypeptide purified from the 2-D gels was blocked at the NH$_2$ terminus, thus was unsuitable for sequencing.

Several studies (Kumagai and Sakai, 1983; Durrieu et al., 1987; Walsh et al., 1989; Launay et al., 1989; Somers et al., 1990) had reported that GAPDH, a homotetramer comprised of 36-kD monomers electrophoresing at basic pI in urea, binds to microtubules. Rabbit muscle GAPDH (Sigma Chemical Co.) was mixed in microgram quantities with radiolabeled microtubule pellets from the CHO cells. The muscle enzyme, detected by staining, and the CHO cell 36-kD polypeptide, detected by fluorography, showed very similar mobilities on 2-D gels (Fig. 5). The relevant spot was excised from the gels, incubated with endoproteinase Glu-C (Calbiochem-Behring Corp.), then electrophoresed. Each of the radiolabeled proteolytic fragments co-electrophoresed with a stained proteolytic fragment from the muscle enzyme (data not shown).

Cloning, Analysis, and Expression of GAPDH cDNA

GAPDH cDNA was prepared from WTB and FD1.3.25 making use of the sequence published for the Syrian hamster enzyme (Vincent and Fort, 1990). The PCR product obtained electrophoresed at 1 kb, the expected length for GAPDH cDNA. As noted above, the 36-kD polypeptide from FD1.3.25 exhibited dominance (or co-dominance) in stable hybrids, raising the possibility that FD1.3.25 might itself be a heterozygote. Thus, prior to undertaking sequencing of GAPDH cDNA from mutant and parent, the cDNA clones were examined for SSCP. Of 19 clones from FD1.3.25, five showed an identical shift in electrophoretic

---

Figure 3. Electron microscopy of WTB and FD1.3.25 following a 30-min pulse with HRP. A photomontage of a representative WTB cell (a) displays no polar clustering of labeled vesicles. (In a the small cluster of labeled vesicles observed at the bottom right belongs to a second cell, a portion of which is located under the cell of interest). An inset of this cell (b) shows medium and small vesicle(s) in the area of the Golgi complex, which itself is unlabeled. Medium and large vesicles from WTB cells are depicted in c and d; note in c the vesicle manifesting a tubular extension, a rare phenomenon in WTB cells. A photomontage of a representative FD1.3.25 cell (e) displays the polar clustering of labeled vesicles commonly observed in these cells; an enlargment of this region is shown in the inset (g) and a similar region from another cell is shown in j. As in the wild type, medium and small labeled vesicles abound in the vicinity of the Golgi complex (f). Various examples of vesicles with tubular extensions, found routinely in FD1.3.25, are shown in h, i, and k–m. N, nucleus. Bars, (a) 2 μm; (b) 0.5 μm; (c and d) 1 μm; (e) 2 μm; (f, g, and j) 1 μm; (h, i, k, l, and m) 0.5 μm.
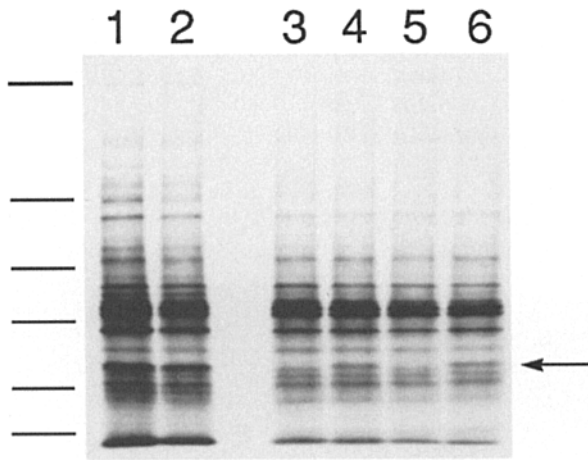
Figure 4. SDS-PAGE of taxol-polymerized microtubules from WTB and FD1.3.25. Cells on one (of four) dishes were labeled overnight with 40 μCi [^{35}S]methionine; label was chased for 20 min prior to harvesting the cells. Microtubules were prepared as described in Materials and Methods; samples corresponding to material obtained from 1/20 of a dish were analyzed on a 4–12% Tris-glycine gel: initial microtubule pellets from WTB (lane *1*) and FD1.3.25 (lane *2*); microtubule pellets washed in 0.4 M NaCl-WTB (lane *3*), FD1.3.25 (lane *4*); microtubule pellets washed in 2 mM ATP-WTB (lane *5*), and FD1.3.25 (lane *6*). The arrow indicates the polypeptide (~36 kD) present in microtubules from the mutant after washing with salt or ATP. Bars denote the positions of molecular weight markers (200, 97.4, 68, 43, 29, and 18.4 kD).

mobility in the 3' one-third of the cDNA; dideoxy-sequencing of these five clones revealed a single nucleotide change, C→T, at nucleotide 700 of the coding sequence, which would result in Pro$_{234}$→Ser. Sequencing of three FD1.3.25 clones that appeared identical to WTB by SSCP showed them to have sequences identical to one another, to that of GAPDH cDNA in WTB clones, and to the sequence reported for Syrian hamster GAPDH.

The nucleotide change reflects an actual mutation in FD1.3.25's GAPDH DNA, rather than an error introduced on PCR amplification. Eleven independent PCR amplifications, initiated with eight independent preparations of either mRNA or total RNA from WTB and FD1.3.25 cells, were assessed by allele specific hybridization. All preparations from WTB hybridized only to the WTB-specific probe, all preparations from FD1.3.25 hybridized to both WTB- and mutant-specific probes. Quantitating results of the hybridization showed that the steady state level of mutant GAPDH RNA in FD1.3.25 is 25 ± 5% of the total GAPDH RNA, in good agreement with our finding that 26% of the cDNA clones initiated with FD1.3.25 mRNA contained the mutation.

To determine whether GAPDH$_{FD}$ was responsible for the altered phenotype of FD1.3.25, parental cells were stably transfected with a mammalian expression vector containing the mutated GAPDH cDNA and a second vector conferring resistance to G418. After selection colonies were picked, amplified and tested for mutant GAPDH RNA by allele specific hybridization following RT-PCR; four of the first seven independent transfectants tested were positive, these were cloned by limiting dilution. Mutant/total GAPDH RNA in one of the cloned transfectants was only 5%; the other three ranged from 12–16% and these were used for further studies.

These transfectants all express the mutant protein. High-speed supernatants prepared from homogenates of the transfectants contained a 36-kD polypeptide that remained bound to taxol-polymerized microtubules after washing with high salt (Fig. 6) or ATP (data not shown). Note that the amounts of bound polypeptide are very similar in the transfectants and FD1.3.25, although the fraction of mutant/total GAPDH RNA in the latter is about twice that measured in the transfectants (see Discussion). GAPDH activity in WTB, FD1.3.25 and the transfectants is identical: 0.44 ± 0.02 U/10^6 cells.

The transfectants closely resemble FD1.3.25 in phenotype. Each exhibits an active ruffle and large vacuoles in the cytoplasm behind the ruffled edge (Fig. 1, *c–e*). As shown in Table II, the transfectants each exhibited increased accumulation of LY. As was observed with FD1.3.25, this appears to result not from increased internalization, but from decreased loss of tracer from late stages of the endocytic pathway. Following a 30-min pulse with LY, labeled endocytic vesicles were found clustered at the poles of the cells (data not shown). Electron microscopic examination of transfectants 1B and 5C following a 30-min pulse with HRP revealed large labeled compartments clustered at one end of the cell as was seen with FD1.3.25 (compare Fig. 7, *a* and *f* with Fig. 4 *e*). As in the mutant, medium-sized endocytic vesicles with tubular projections were commonplace in the transfectants (Fig. 7, *c–e*, *g*, and *i–m*).

Discussion

The results of this study show that a single amino acid substitution in a minor (15–25%) fraction of CHO cells'

Table II. Comparison of Endocytic Activities in WTB and WTB-GAPDH$_{FD}$ Stable Transfectants

	WTB	1B	5C	9C
HRP internalization*				
6 min	6.8 ± 0.6	7.0 ± 0.3	6.6 ± 0.6	7.1 ± 0.7
30 min	23.8 ± 1.2	29.4 ± 1.6	28.9 ± 1.0	31.2 ± 2.4
LY Recycling‡				
30-min pulse	1	1.3 (1.1–1.5)	1.2 (1.0–1.5)	1.3 (1.1–1.6)
90-min chase	0.48 (0.28–0.59)	1.1 (0.8–1.4)	0.9 (0.8–1.2)	1.0 (0.7–1.3)

*Results presented are from three experiments with duplicate samples for each time point. Values given, corrected for background as described, represent ng HRP/100 μg cell protein.
‡Results presented are from three experiments each of which contained WTB and a pair of tranfectants; values presented reflect measurements from 88 WTB cells, and from 60 cells of each transfectant and are normalized as described in Table I. Values in parentheses represent the range obtained with individual cells, normalized to the corresponding wild type cell in the pulse sample, again as described in Table I.
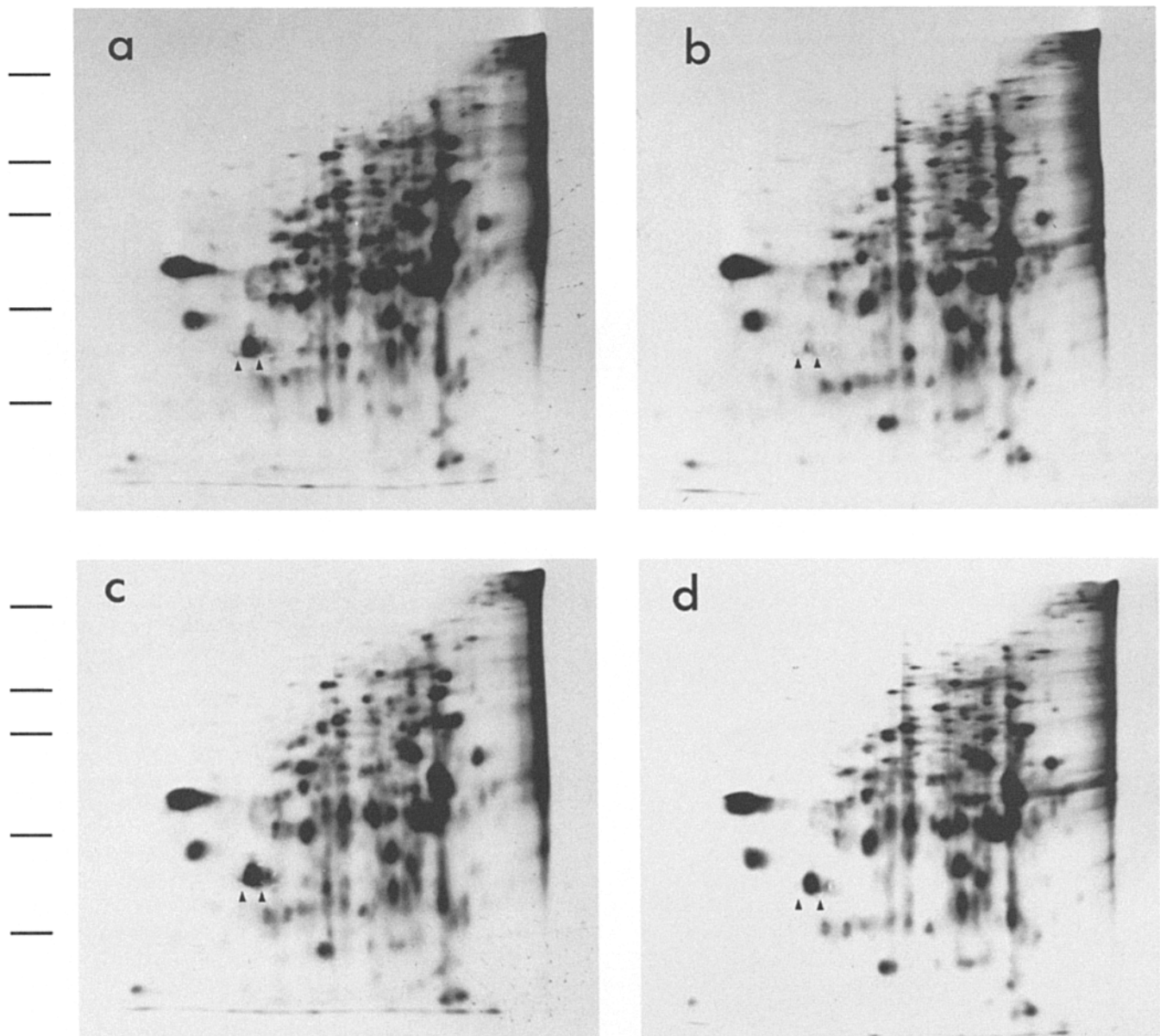
Figure 5. 2-D gel electrophoresis of untreated and salt-washed taxol-polymerized microtubules from WTB and FD1.3.25; co-electrophoresis with rabbit muscle GAPDH. Cells on one (of eight) dishes were labeled overnight as described in the legend to Fig. 4. Prior to electrophoresis 3 mg of rabbit muscle GAPDH was added to each sample of taxol-polymerized microtubules; samples corresponded to the material obtained from 2/5 of one dish. 2-D gel electrophoresis was conducted as described in Materials and Methods; the basic end of the first dimension gel corresponds to the left side of each panel: initial microtubule pellets from WTB (*a*) and FD1.3.25 (*c*); salt washed microtubule pellets from WTB (*b*) and FD1.3.25 (*d*). Rabbit muscle GAPDH was detected by staining the gels with Coomassie blue, polypeptides from the microtubule preparations by subsequent fluorography. The muscle enzyme showed four isoforms, all electrophoresing at ∼36 kD, that decreased in staining intensity from basic to acidic. The initial microtubule pellet from WTB (*a*) and both the initial (*c*), and salt-washed (*d*) microtubule pellets from FD1.3.25 exhibit a polypeptide electrophoresing between the two major isoforms of the rabbit muscle GAPDH, the positions of which are shown by arrowheads; close examination reveals the pinholes used to mark these spots on the gels prior to fluorography. Parallel samples of the taxol-polymerized microtubules were electrophoresed without added GAPDH; no Coomassie staining was observed in the 36-kD region; comparison of the fluorographs from gels with and without added enzyme showed no differences in the mobilities of radiolabeled polypeptides (data not shown). Bars denote the positions of molecular weight markers (200, 100, 69, 46, and 30 kD).

GAPDH polypeptides effects several phenotypic changes. In terms of cell morphology, cells expressing GAPDH$_{FD}$ exhibit a prominent ruffle at one edge with numerous unidentified vacuoles in the cytoplasm behind the ruffle (Fig. 1). The net effect of the mutant enzyme on endocytosis is increased accumulation of fluid phase tracers, apparently due to decreased retroendocytosis of tracers from late endocytic compartments (Tables I and II); no difference was observed between parent and mutant with respect to either initial rates of fluid phase tracer internalization or ki-
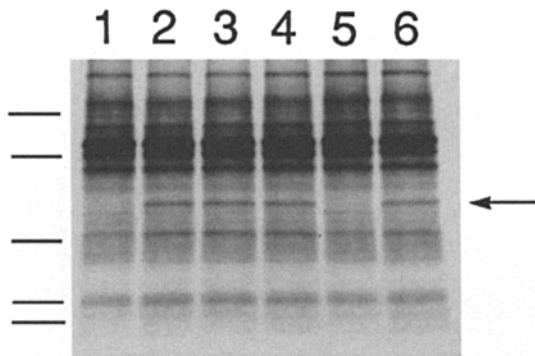
Figure 6. Taxol-polymerized microtubules from WTB-GAPDH$_{FD}$ stable transfectants. Cells on one (of two) dishes were labeled with [^{35}S]methionine as described in the legend to Fig. 4. Microtubule pellets were washed with 0.4 M NaCl; samples corresponding to 1/10 of a dish were analyzed by SDS-PAGE on an 8–16% Tris-glycine gel: WTB (lanes *1* and *5*); transfectants 1B (lane *2*), 5C (lane *3*), and 9C (lane *4*); FD1.3.25 (lane *6*). The arrow shows the position of the 36-kD polypeptide (GAPDH); bars indicate positions of molecular weight markers (69, 46, 30, 21.5, and 14.3 kD).

netics of transferrin recycling. Examination by electron microscopy showed HRP, a fluid phase tracer, and transferrin-HRP present in wild type, mutant, and transfectants in small vesicles and tubular structures of similar appearance and distribution, concentrated in the vicinity of the Golgi complex. However, in cells expressing GAPDH$_{FD}$, HRP, but not transferrin-HRP, was also found in unusual 400 nm vesicles characterized by tubular extensions (Figs. 3 and 7). These compartments resemble CURL (compartment of uncoupling of receptor and ligand; Geuze et al., 1983), or sorting endosomes (Yamashiro et al., 1984), albeit their lack of transferrin indicates that they are a later compartment. Observed at the light level, fluid phase tracers appear to move more rapidly to the ends of cells expressing the mutant enzyme (Fig. 2). Electron microscopy revealed an accumulation of large HRP-containing vesicles clustered at one pole of these cells (Figs. 3 and 7).

In GAPDH$_{FD}$ Ser replaces Pro$_{234}$; this Pro is a member of the tetrapeptide ArgValProThr that is present in GAPDH from every species (bacteria, yeast, fungi, plants, and animals) examined to date. From analysis of the crystal structure of the lobster enzyme, Moras et al. (1975) deduced that Pro$_{234}$ is involved in several intersubunit contacts, and that its position is strongly influenced by that of His$_{176}$, involved in formation of the thio-hemiacetal intermediate. Results of ongoing studies of bacterially expressed GAPDH have shown that while GAPDH$_{FD}$ homotetramers are enzymatically active, their activity is sensitive to a variety of perturbations that are without effect on GAPDH$_{WT}$ (Hall, C. W., and A. R. Robbins, unpublished results). Given that RNA encoding GAPDH$_{FD}$ is ≤25% of the total GAPDH RNA, few homotetramers of GAPDH$_{FD}$ are likely to be present in the mutant and transfectants. In vitro studies of the enzyme will be extended to multimers comprised of normal and mutant subunits; it is hoped that these experiments will resolve the disparity observed between levels of GAPDH$_{FD}$ RNA and amounts of GAPDH polypeptide bound to taxol-polymerized microtubules (Fig. 6). It may be that a single GAPDH$_{FD}$ monomer per

tetramer is sufficient to achieve altered binding; alternatively, tetramers containing more than one GAPDH$_{FD}$ may be unstable and go undetected in our assay.

How might GAPDH$_{FD}$ effect the changes in endocytosis we observe? Reducing the endocytic pathway to simplest form, any of three models could account for increased accumulation. In each of these models it is assumed that recycling from lysosomes is less than that from earlier compartments. Model 1. The normal pathway is circumvented; i.e., fluid phase tracers bypass early compartments, proceeding directly to lysosomes. Model 2. Forward (toward the lysosome) movement of tracer proceeds normally, but backward movement is inhibited. Model 3. Forward movement is accelerated, so tracer spends less time in compartments that actively recycle.

Regarding model 1, macropinocytosis seemed an attractive possibility given the increased ruffling and large vacuoles consequent to expression of GAPDH$_{FD}$. Two quite different pictures of macropinocytosis have emerged from studies of two cell types: in A431 cells stimulated with EGF, the macropinocytic pathway appeared totally distinct from the coated pit pathway; tracer internalized via macropinosomes was eliminated from the cells by exocytosis 2 h after internalization (Hewlett et al., 1994). But, in macrophages stimulated with macrophage colony stimulating factor, the coated pit and macropinocytic pathways were shown to converge after the early endosome (Racoosin and Swanson, 1992, 1993). Because cells with GAPDH$_{FD}$ exhibit increased, not decreased, accumulation on long chases, we can eliminate A431-like macropinocytosis as an explanation for our results. On the other hand, a macrophage-like pathway in which fluid phase tracer bypassed earlier compartments en route to lysosomes would be consistent with our findings. However, the vacuoles in cells with GAPDH$_{FD}$ did not contain endocytic tracer, and cells with GAPDH$_{FD}$ did not exhibit increased internalization of HRP (Tables I and II) as would be expected if endocytosis via macropinocytosis were added to that occurring through coated pits. Thus, any macropinocytic uptake would have to be balanced by a decrease in uptake via coated pits. We observed no decrease using either transferrin (Table I) or lysosomal enzymes (data not shown) as ligands.

Decreased backward movement of tracer (model 2) could reflect either inhibition of budding of recycling vesicles from late endosomes or lysosomes (model 2A), or decreased fusion of those vesicles with their target organelles (model 2B). Inhibition of vesicle budding is an appealing hypothesis, in light of the tubulo-vesicular, HRP-containing 400 nm compartments characteristic of cells expressing GAPDH$_{FD}$. There are several precedents for inhibition of vesicle budding resulting in tubularization. In temperature-sensitive *shibire* mutants of *Drosophila*, pinching off of endocytic vesicles from plasma membrane coated pits is blocked, resulting in elongated tubules extending inward from the membrane (Narita et al., 1989). In brefeldin A–treated cells, budding of vesicles from the Golgi and *trans*-Golgi network is inhibited, resulting in tubularization of those organelles (Klausner et al., 1992). Interestingly, brefeldin A has been shown to stimulate ADP-ribosylation of two proteins, one of which is GAPDH (De Matteis et al., 1994). Regarding model 2B, GAPDH has been shown to be an
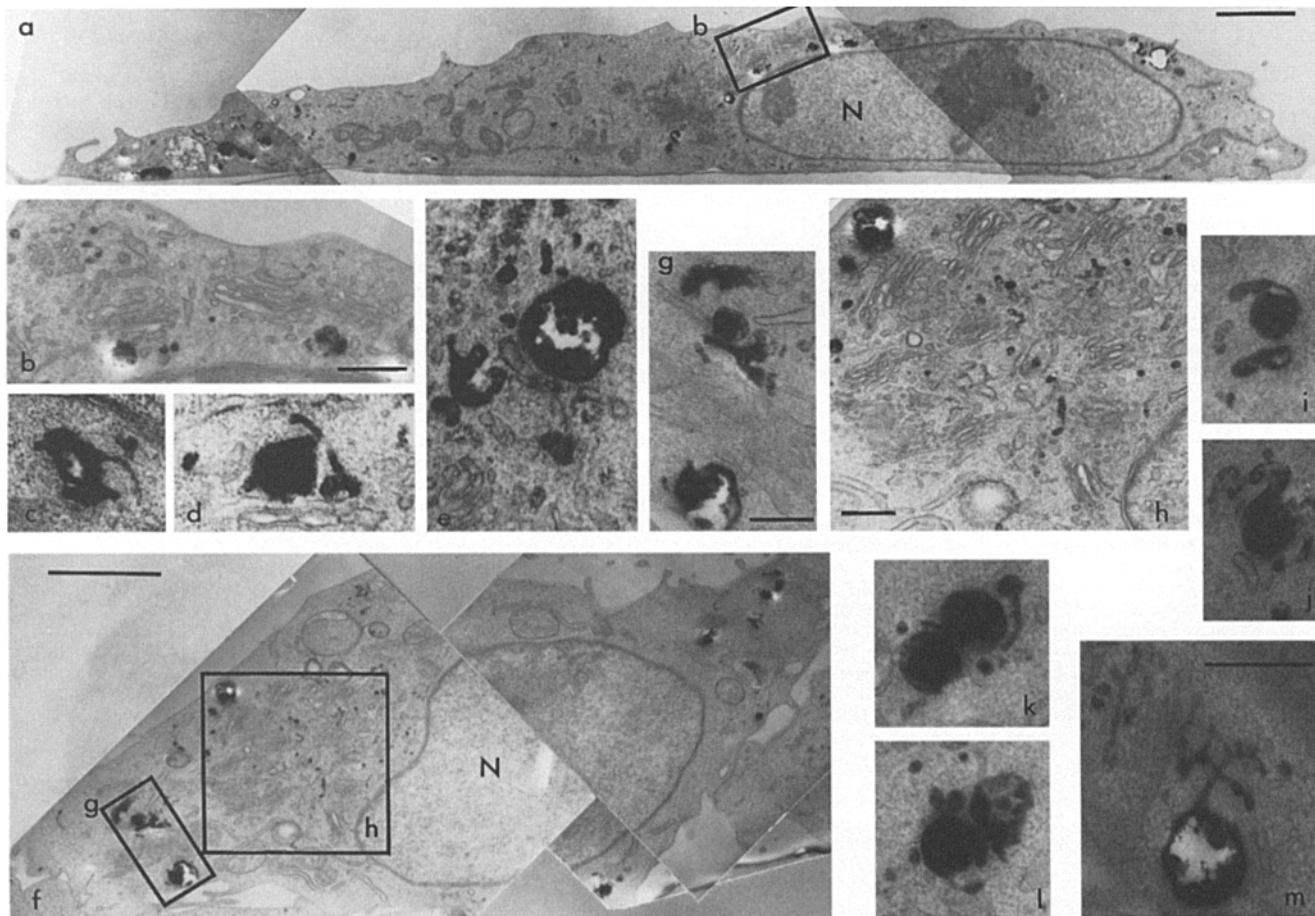
Figure 7. Electron microscopy of WTB-GAPDH$_{FD}$ stable transfectants 1B and 5C, following a 30-min pulse with HRP. Representative 1B (*a*) and 5C (*f*) cells display polar clusters of labeled vesicles in the tapered ends of the cells. Inset (*g*) shows a higher magnification of the cluster from 5C. Insets (*b*) and (*h*) show show small labeled vesicles interspersed throughout the region of the Golgi complex. Representative medium-sized vesicles with tubular projections from 1B cells are presented in micrographs (*c–e*), and those from 5C are presented in (*i–m*). Note the extensive tubular network found in (*m*). *N*, nucleus. Bars, (*a* and *f*) 2 μm; (*b*, *g*, and *h*) 0.5 μm; the bar in *m*, refers to *c–e* and *i–m*, 0.5 μm.

effective fusogen in systems employing phospholipid vesicles (López-Vinals et al., 1987). GAPDH$_{FD}$ may be decreased in this activity. A caveat regarding model 2B is that the thwarted recycling vesicles must re-enter the forward moving endocytic pathway, because on cell fractionation we observed no accumulation of tracer in FD1.3.25 at other than lysosomal densities.

Model 3, invoking increased forward movement of tracer, is similar to that proposed to explain decreased exocytosis of internalized tracer from macrophages manifesting tubular lysosomes (Swanson et al., 1985, 1987a). The tubular structure of lysosomes was hypothesized to promote more efficient transfer of solute from a compartment that rapidly filled and emptied into a compartment that emptied more slowly. Maintenance of tubular lysosomes in macrophages depends on intact microtubules (Swanson et al., 1987b). That GAPDH$_{FD}$ affects the interaction of late endocytic compartments with microtubules is consistent with sequestration of 0.8–1.3 μm HRP-containing compartments at the cell poles in FD1.3.25 (Figs. 2 and 3) and transfectants (Fig. 7), the altered association of GAPDH$_{FD}$ with microtubules in vitro (Figs. 4–6), the disappearance of the 400 nm tubular endocytic compart-

ments upon microtubule depolymerization and, following shifts in cytoplasmic pH, the increased outward movement of late endocytic compartments in cells with GAPDH$_{FD}$ (manuscript in preparation). This model holds the added attraction of invoking a gain, rather than a loss of function associated with GAPDH$_{FD}$. The former is easier to reconcile with phenotypic expression in cells that, based on RNA levels, contain only one monomer of GAPDH$_{FD}$ for every five monomers of GAPDH$_{WT}$.

References

Arnold, H., and D. Pette. 1970. Binding of aldolase and triosephosphate dehydrogenase to F-actin and modification of catalytic properties of aldolase. *Eur. J. Biochem.* 15:360–366.

Bonner, W. M., and R. A. Laskey. 1974. A film detection method for tritium-labeled proteins and nucleic acids in polyacrylamide gels. *Eur. J. Biochem.* 46:83–88.

Brandt, N. R., A. H. Caswell, S.-R. Wen, and J. A. Talvenheimo. 1990. Molecular interactions of the junctional foot protein and dihydropyridine receptor in skeletal muscle triads. *J. Memb. Biol.* 113:237–251.

Cabral, F., and M. M. Gottesman. 1978. The determination of similarities in amino acid composition among proteins separated by two-dimensional gel electrophoresis. *Anal. Biochem.* 91:548–556.

Caswell, A. H., and A. C. Corbett. 1985. Interaction of glyceraldehyde-3-phosphate dehydrogenase with isolated microsomal subfractions of skeletal muscle. *J. Biol. Chem.* 260:6892–6898.

Cool, B. L., and M. A. Sirover. 1989. Immunocytochemical localization of the base excision repair enzyme uracil DNA glycosylase in quiescent and proliferating normal human cells. *Cancer Res.* 49:3029–3036.

De Matteis, M. A., M. Di Girolamo, A. Colanzi, M. Pallas, G. Di Tullio, L. McDonald, J. Moss, G. Santini, S. Bannykh, D. Corda, and A. Luini. 1994. Stimulation of endogenous ADP-ribosylation by brefeldin A. *Proc. Natl. Acad. Sci. USA.* 91:1114–1118.

Doucet, J.-P., and B. S. Tuana. 1991. Identification of low molecular weight GTP-binding proteins and their sites of interaction in subcellular fractions from skeletal muscle. *J. Biol. Chem.* 266:17613–17620.

Durrieu, C., F. Bernier-Valentin, and B. Rousset. 1987. Microtubules bind glyceraldehyde 3-phosphate dehydrogenase and modulate its enzyme activity and quaternary structure. *Arch. Biochem. Biophys.* 252:32–40.

Ercolani, L., D. Brown, A. Stuart-Tilley, and S. L. Alper. 1992. Colocalization of GAPDH and band 3 (AE1) proteins in rat erythrocytes and kidney intercalated cell membranes. *Am. J. Physiol.* 262:F892–F896.

Geuze, H. J., J. W. Slot, G. J. Strous, H. F. Lodish, and A. L. Schwartz. 1983. Intracellular site of asialoglycoprotein receptor ligand uncoupling: double-label immunoelectron microscopy during receptor-mediated endocytosis. *Cell.* 32:277–287.

Heuser, J. 1989. Changes in lysosome shape and distribution correlated with changes in cytoplasmic pH. *J. Cell Biol.* 108:855–864.

Hewlett, L. J., A. R. Prescott, and C. Watts. 1994. The coated pit and macropinocytic pathways serve distinct endosome populations. *J. Cell Biol.* 124:689–703.

Klausner, R. D., J. G. Donaldson, and J. Lippincott-Schwartz. 1992. Brefeldin A: insights into the control of membrane traffic and organelle structure. *J. Cell Biol.* 116:1071–1080.

Klausner, R. D., J. van Renswoude, C. Kempf, K. Rao, J. L. Bateman, and A. R. Robbins. 1984. Failure to release iron from transferrin in a Chinese hamster ovary cell mutant pleiotropically defective in endocytosis. *J. Cell Biol.* 98:1098–1101.

Kliman, H. F., and T. L. Steck. 1980. Association of glyceraldehyde 3-phosphate dehydrogenase with the human red cell membrane. A kinetic analysis. *J. Biol. Chem.* 255:6314–6321.

Kozak, M. 1987. An analysis of 5'-noncoding sequences from 699 vertebrate messenger RNAs. *Nucleic Acid Res.* 15: 8125–8132.

Kumagai, H., and H. Sakai. 1983. A porcine brain protein (35 k protein) which bundles microtubules and its identification as glyceraldehyde 3-phosphate dehydrogenase. *J. Biochem.* 93:1259–1269.

Lachaal, M., C. J. Berenski, J. Kim, and C. Y. Jung. 1990. An ATP-modulated specific association of glyceraldehyde-3-phosphate dehydrogenase with human erythrocyte glucose transporter. *J. Biol. Chem.* 265:15449–15454.

Launay, J. F., A. Jellali, and M. T. Vanier. 1989. Glyceraldehyde-3-phosphate dehydrogenase is a microtubule binding protein in a human colon tumor cell line. *Biochim. Biophys. Acta.* 996:103–109.

López-Vinals, A. E., R. N. Farias, and R. D. Morero. 1987. Characterization of the fusogenic properties of glyceraldehyde-3-phosphate dehydrogenase: fusion of phospholipid vesicles. *Biochem. Biophys. Res. Commun.* 143:403–409.

Marchuk, D., M. Drumm, A. Saulino, and F. S. Collins. 1991. Construction of T-vectors, a rapid and general system for direct cloning of unmodified PCR products. *Nucleic Acid Res.* 19:1154.

Méjean, C., F. Pons, Y. Benyamin, and C. Roustan. 1989. Antigenic probes locate binding sites for the glycolytic enzymes glyceraldehyde-3-phosphate dehydrogenase, aldolase and phosphofructokinase on the actin monomer in microfilaments. *Biochem. J.* 264:671–677.

Minaschek, G., U. Gröschel-Stewart, S. Blum, and J. Bereiter-Hahn. 1992. Microcompartmentation of glycolytic enzymes in cultured cells. *Eur. J. Cell Biol.* 58:418–428.

Moras, D., K. W. Olsen, M. N. Sabesan, M. Buehner, G. C. Ford, and M. G.

Rossmann. 1975. Studies of asymmetry in the three-dimensional structure of lobster D-glyceraldehyde-3-phosphate dehydrogenase. *J. Biol. Chem.* 250: 9137–9162.

Morgenegg, G., G. C. Winkler, U. Hübscher, C. W. Heizmann, J. Mous, and C. C. Kuenzle. 1986. Glyceraldehyde-3-phosphate dehydrogenase is a non-histone protein and a possible activator of transcription in neurons. *J. Neurochem.* 47:54–62.

Mullis, K. B., and F. A. Faloona. 1987. Specific synthesis of DNA *in vitro* via a polymerase-catalyzed chain reaction. *Methods Enzymol.* 155:335–350.

Myerowitz, R. 1988. Splice junction mutation in some Ashkenazi Jews with Tay-Sachs disease: evidence against a single defect within this ethnic group. *Proc. Natl. Acad. Sci. USA.* 85:3955–3959.

Narita, K., T. Tsuruhara, J. H. Koenig, and K. Ikeda. 1989. Membrane pinch-off and reinsertion observed in living cells of *Drosophila. J. Cell. Physiol.* 141: 383–391.

O'Farrell, P. H. 1975. High resolution two-dimensional electrophoresis of proteins. *J. Biol. Chem.* 250:4007–4021.

O'Farrell, P. Z., H. M. Goodman, and P. H. O'Farrell. 1977. High resolution two-dimensional electrophoresis of basic as well as acidic proteins. *Cell.* 12: 1133–1142.

Orita, M., Y. Suzuki, T. Sekiya, and K. Hayashi. 1989. Rapid and sensitive detection of point mutations and DNA polymorphisms using the polymerase chain reaction. *Genomics.* 5:874–879.

Racoosin, E. L., and J. A. Swanson. 1992. M-CSF-induced macropinocytosis increases solute endocytosis but not receptor-mediated endocytosis in mouse macrophages. *J. Cell Sci.* 102:867–880.

Racoosin, E. L., and J. A. Swanson. 1993. Macropinosome maturation and fusion with tubular lysosomes in macrophages. *J. Cell Biol.* 121:1011–1020.

Robbins, A. R., C. Oliver, J. L. Bateman, S. S. Krag, C. J. Galloway, and I. Mellman. 1984. A single mutation in Chinese hamster ovary cells impairs both Golgi and endosomal functions. *J. Cell Biol.* 99:1296–1308.

Sanger, F., S. Nicklen, and A. R. Coulson. 1977. DNA sequencing with chain-terminating inhibitors. *Proc. Natl. Acad. Sci. USA.* 74:5463–5467.

Siegler, K. M., D. J. Mauro, G. Seal, J. Wurzer, J. K. deRiel, and M. A. Sirover. 1991. A human nuclear uracil DNA glycosylase is the 37-kDa subunit of glyceraldehyde-3-phosphate dehydrogenase. *Proc. Natl. Acad. Sci. USA.* 88: 8460–8464.

Singh, R., and M. R. Green. 1993. Sequence-specific binding of transfer RNA by glyceraldehyde-3-phosphate dehydrogenase. *Science (Wash. DC).* 259: 365–368.

Somers, M., Y. Engelborghs, and J. Baert. 1990. Analysis of the binding of glyceraldehyde-3-phosphate dehydrogenase to microtubules, the mechanism of bundle formation and the linkage effect. *Eur. J. Biochem.* 193:437–444.

Spurr, A. R. 1969. A low viscosity epoxy resin embedding medium for electron microscopy. *J. Ultrastruct. Res.* 26:31–43.

Struhl, K. 1985. A rapid method for creating recombinant DNA molecules. *BioTechniques.* 3:452–453.

Swanson, J., E. Burke, and S. C. Silverstein. 1987a. Tubular lysosomes accompany stimulated pinocytosis in macrophages. *J. Cell Biol.* 104:1217–1222.

Swanson, J., A. Bushnell, and S. C. Silverstein. 1987b. Tubular lysosome morphology and distribution within macrophages depend on the integrity of cytoplasmic microtubules. *Proc. Natl. Acad. Sci. USA.* 84:1921–1925.

Swanson, J. A., B. D. Yirinec, and S. C. Silverstein. 1985. Phorbol esters and horseradish peroxidase stimulate pinocytosis and redirect the flow of pinocytosed fluid in macrophages. *J. Cell Biol.* 100:851–859.

Takebe, Y., M. Seiki, J.-I. Fujisawa, P. Hoy, K. Yokota, K.-I. Arai, M. Yoshida, and N. Arai. 1988. SRα promoter: an efficient and versatile mammalian cDNA expression system composed of the simian virus 40 early promoter and the R-U5 segment of human T-cell leukemia virus type 1 long terminal repeat. *Mol. Cell. Biol.* 8:466–472.

Thompson, L. H., and R. M. Baker. 1973. Isolation of mutants in mammalian cells. *Methods Cell Biol.* 6:209–281.

Vallee, R. B. 1982. A taxol-dependent procedure for the isolation of microtubules and microtubule-associated proteins. *J. Cell Biol.* 92:435–442.

van den Hoff, M. J. B., A. F. M. Moorman, and W. H. Lamers. 1992. Electroporation in "intracellular" buffer increases cell survival. *Nucleic Acid Res.* 20: 2902.

Vincent, S., and P. Fort. 1990. Nucleotide sequence of hamster glyceraldehyde-3-phosphate dehydrogenase mRNA. *Nucleic Acid Res.* 18:3054.

Walsh, J. L., T. J. Keith, and H. R. Knull. 1989. Glycolytic enzyme interactions with tubulin and microtubules. *Biochim. Biophys. Acta.* 999:64–70.

West, M. A., M. S. Bretscher, and C. Watts. 1989. Distinct endocytic pathways in epidermal growth factor-stimulated human carcinoma A431 cells. *J. Cell Biol.* 109:2731–2739.

Yamashiro, D. J., B. Tycko, S. R. Fluss, and F. R. Maxfield. 1984. Segregation of transferrin to a mildly acidic (pH 6.5) para-Golgi compartment in the recycling pathway. *Cell.* 37:769–800.